Title

Molecular Brush Surfactants: Versatile Emulsifiers for Stabilizing and Structuring Liquids

Journal

Angewandte Chemie International Edition, 60(36)

ISSN

1433-7851

Authors

Wang, Beibei

Liu, Tan

Chen, Hao

et al.

Publication Date

2021-09-01

DOI

10.1002/anie.202104653

Molecular Brush Surfactants: Versatile Emulsifiers for Stabilizing and Structuring Liquids

Beibei Wang, [a] Tan Liu, [a] Hao Chen, [a] Bangqi Yin, [a] Zhao Zhang, [a] Thomas P. Russell, [b, c] and Shaowei Shi*[a]

[a] B. Wang, T. Liu, H. Chen, B. Yin, Z. Zhang, Prof. S. Shi
Beijing Advanced Innovation Center for Soft Matter Science and Engineering, College of Materials Science and Engineering, Beijing University of Chemical Technology, Beijing 100029, China
E-mail: shisw@mail.buct.edu.cn
[b] Prof. T. P. Russell
Department of Polymer Science and Engineering, University of Massachusetts, Amherst, Massachusetts 01003, USA
[c] Prof. T. P. Russell
Materials Sciences Division, Lawrence Berkeley National Laboratory, 1 Cyclotron Road, Berkeley, California 94720, USA

Supporting information for this article is given via a link at the end of the document.

Abstract: Using amphiphilic molecular brushes to stabilize emulsions usually requires the synthesis of specific side chains, which can be a time-consuming and difficult challenge to meet. By taking advantage of the electrostatic interactions between water-soluble molecular brushes and oil-soluble oligomeric ligands, the *in-situ* formation, assembly and jamming of molecular brush surfactants (MBSs) at the oil-water interface is described. With MBSs, stable emulsions including o/w, w/o and o/w/o can be easily prepared by varying the molar ratios of the molecular brush to the ligands. Moreover, when jammed, the binding energy of MBSs at the interface is sufficiently strong to allow the stabilization of liquids in nonequilibrium shapes, i.e., structuring liquids, producing an elastic film at the interface with exceptional mechanical properties. These structured liquids have numerous potential applications in fields of chemical biphasic reactions, liquid electronics, and all-liquid biomimetic system.

Emulsions have been widely studied and applied in a broad range of fields, including pharmaceutics, cosmetics, and food industries.[1-5] In general, amphiphilic small molecules, linear diblock copolymers, and colloidal particles are used as emulsifiers to stabilize the liquid-liquid interface, reducing the interfacial energy and preventing the coalescence between emulsion droplets.[6-8] By fine-tuning the hydrophilic-lipophilic balance of the emulsifiers at the interface or the volume ratios of the two liquids, different types of emulsions, e.g., oil-in-water (o/w) and water-in-oil (w/o) emulsion can be achieved.[9] Recently, a newly developed emulsifier, termed a nanoparticle surfactant, formed by the interactions between nanoparticles and polymeric/oligomeric ligands at the oil-water interface, has shown promising potentials in stabilizing emulsion droplets and, more attractively, locking the shape of the liquids in nonequilibrium shapes by the interfacial jamming of the nanoparticle surfactants at the interface.[10-13] By taking advantage of nanoparticle surfactants, liquids can be processed into arbitrary shapes, using liquid molding or all-liquid 3D printing strategies, opening a pathway to fabricate complex, reconfigurable liquid devices for mass or ion transport, compartmentalized reactions, and encapsulation.[14-18] This cooperative assembly approach is universal, and can be applied to nanoparticles of different sizes, shapes, and chemical compositions. For example, spherical silica NPs (0D),[19-20] cellulose nanocrystals (1D),[21-22] and MXenes/graphene oxides (2D)[23-25] have been used to generate nanoparticle surfactants to structure liquids.

Among the numerous nanomaterials, molecular brushes (MB), polymers having numerous polymeric side chains that are densely grafted to a macromolecular backbone, have attracted attention due to their unique molecular architecture.[26-29] Unlike linear polymers that are entangled, the steric crowding of the side chains in the molecular brushes stiffen the backbone, leading to the formation of cylindrical nanostructures with lengths that can exceed hundreds of nanometers.[30] A broad variety of structural diversity can be achieved with molecular brushes. The grafting density, side-chain/backbone length, as well as the chemical composition can be tailored to meet specific demands.[30] By grafting both hydrophobic and hydrophilic side-chains to the backbone, the amphiphilic MB can behave as a polymeric surfactant to stabilize emulsions, with higher emulsifying efficiencies in comparison to their linear diblock analogues (Figure 1a).[31-32] Less attention, though, has been given to amphiphilic molecular brushes, due, in part, to the chemical specificity and the lineal densities of the side-chains needed to ensure solubility of the resultant MB in either the oil or water phase.[33-35] This complicates the synthesis of the MBs and limits their application.

Here, we report a simple and versatile strategy to generate molecular brush surfactants (MBSs) at the oil-water interface, using interfacial interactions between a hydrophilic MB in the aqueous phase and hydrophobic ligands in the oil phase (Figure 1b). A “Janus-type” MBSs forms *in-situ* at the interface, significantly reducing the interfacial energy. The “Janus-type” MBSs are very efficient emulsifiers that stabilize o/w and w/o emulsions and, unexpectedly, multiple emulsions. Due to the increased rigidity of the backbone chain and the high binding energy of MBSs at the interface, a jamming

MBSs at the interface occurs at the interfaces when the interfacial area is decreased, leading to robust assemblies with exceptional mechanical properties that stabilize nonequilibrium liquid shapes (Figure 1c).

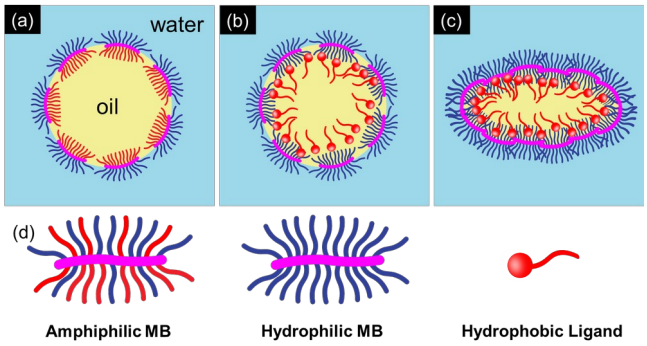

Figure 1. Schematic representation of a spherical droplet stabilized by (a) amphiphilic MB and (b) MBS. (c) Schematic representation of a droplet in a nonequilibrium shape, with MBSs jammed at the interface. (d) Schematic representation of amphiphilic MB, hydrophilic MB and hydrophobic ligand.

As a proof-of-concept, we use poly(2-hydroxyethyl methacrylate)-*g*-poly(acrylic acid) (PHEMA-*g*-PAA) and amine-functionalized polyhedral oligomeric silsesquioxane (POSS-NH_2) to generate MBSs at the toluene-water interface (Figure 2a). A detailed synthesis of PHEMA-*g*-PAA is given in the Supporting Information (Scheme S1, Figure S1-S4). The grafting ratio of PAA side chains is ~90%, and the length of cylindrical PHEMA-*g*-PAA is several hundreds of nanometers, with a diameter of ~30 nm (Figure S5). MB-90 designates PHEMA-*g*-PAA with 90% grafting ratio of PAA side chains. Prior to investigating the kinetics of the MBS formation and assembly at the toluene-water interface, the effect of pH on the interfacial activity of MB-90 and POSS-NH_2 is systematically studied. As shown in Figure 2b-c, with MB-90 dissolved in water against pure toluene, weak interfacial activity is observed at higher pH (> 7.0), with an equilibrium interfacial tension of ~34 mN m^{-1}, close to that of the pure toluene-water system (~36 mN m^{-1}). As the pH decreases, a gradual reduction in the interfacial tension is obtained, indicating an increased interfacial activity of MB-90. Since MB-90 is rich in carboxylic acid groups, at lower pH, the degree of protonation of the carboxylic acid groups increases, leading to the enhanced hydrophobicity of MB-90 and, therefore, the spontaneous segregation of MB-90 at the toluene−water interface (Figure 2b). For POSS-NH_2 dissolved in toluene against pure water, the relatively low interfacial tension over a wide pH range (2.0-8.0) indicates the surfactant nature of POSS-NH_2 (Figure S6). As the pH decreases, an enhanced interfacial activity of POSS-NH_2 is also observed due to the increased degree of protonation of the amine groups and enhanced hydrophilicity. However, when the interfacial assemblies of either PHEMA-*g*-PAA or POSS-NH_2 are com-pressed, no wrinkling is observed, indicating that the binding energies of MB-90 and POSS-NH_2 are not sufficient to with-stand the compressive force, and the molecules are ejected from the interface (Video S1).

The pH dependence of the interfacial activity of the MBSs is manifest in the behavior of MB-90 dissolved in water against POSS-NH_2 dissolved in toluene, and is dictated by the carboxylate-ammonium ion pairing. As shown in Figure 2d-e, by decreasing pH from 9.0 to 3.0, a reduction in the interfacial tension from ~28 to extremely low ~4 mN m^{-1} is observed, indicating the formation and assembly of MBSs at the interface, significantly decreasing the interfacial energy. At a pH of 3.0, when the volume, and, therefore, interfacial area of the droplet is reduced to compress the interfacial assembly, a wrinkling of the interface is observed, indicating a jamming of the MBS assembly and the "solid-like" characteristics of the assembly (Video S2). We note that no relaxation of wrinkles is observed, due to the mechanical strength of the interface (Figure S7). These results give strong evidence that the binding energy of MB-90 is markedly increased due to the interfacial interactions with POSS-NH_2. The surface coverage of MBSs decreases with the increasing pH, which is related to the interfacial activity of MBSs (Figure 2e). As shown in Figure 2f, by increasing pH, both MB-90 and POSS-NH_2 are less protonated, weakening the electrostatic interactions and suppressing the formation of MBSs at the interface. By varying the concentration of either MB-90 or POSS-NH_2, the interfacial activity, as well as the surface coverage of MBSs can be adjusted, as shown in Figure S8. In the following experiments, the pH of the aqueous phase is fixed at 3.0, to ensure that the interfacial activity and surface coverage of the MBSs are sufficiently high for the generation of all-liquid constructs, including emulsions and structured liquids.

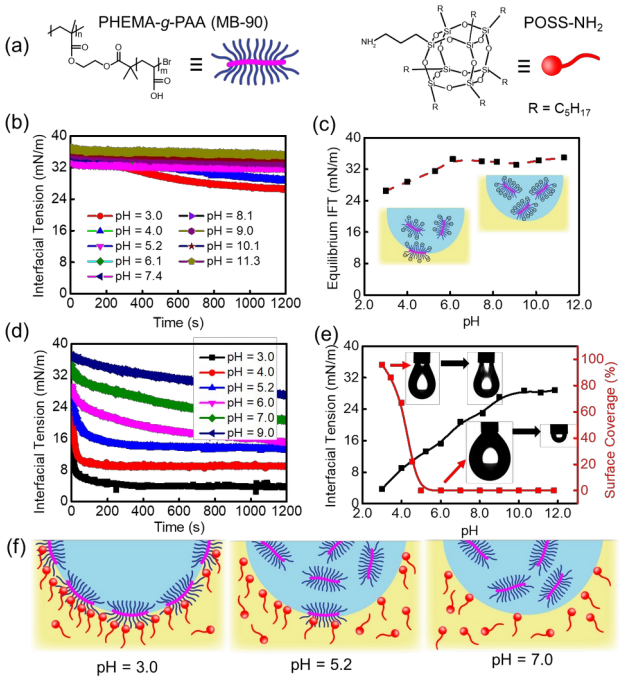

Figure 2. (a) Chemical structures of the PHEMA-*g*-PAA (MB-90) and POSS-NH_2. (b) Time evolution of interfacial tension and (c) equilibrium interfacial tension between MB-90 aqueous solution and pure toluene with different pH values. [MB-90] = 0.1 mg mL^{-1}. (d) Time evolution of the interfacial tension and (e) equilibrium interfacial tension between MB-90 aqueous solution and POSS-NH_2 toluene solution with different pH values. [MB-90] = 0.1 mg mL^{-1},

[POSS-NH_2] = 0.1 mg mL^{-1}. (f) Schematic representation of the interfacial activity of MBSs with different pH values.

To understand the robust nature of the interfacial assemblies formed by MBSs, linear PAA (L-PAA, M_w = 2.0 K) was used as a control to interact with POSS-NH_2 at the interface. As shown in Figure S9, with L-PAA dissolved in water against POSS-NH_2 dissolved in toluene, the interfacial tension decreases to ~5 mN m^{-1}, similar to that seen for the toluene-water system having MBSs at the interface. However, when the droplet is compressed, no wrinkling is observed, indicating the binding energy of linear PAA is too low to support the compressive load at the interface (Figure 3a and Video S3). In comparison to MBSs with a cylindrical nanostructure, L-PAA is a random coil in the aqueous phase with a much smaller characteristic size at the interface, and the reduction in the interfacial energy for each L-PAA chain is very low. As a result, L-PAA easily desorbs from the interface even with electrostatic interactions between PAA and POSS-NH_2, and the interface exhibits "liquid-like" characteristics. The mechanical properties of the interfacial assemblies can also be adjusted by varying the grafting ratio of the side chain. As shown in the atomic force microscope images (Figure S5), in comparison to MB-90, MB-40, PHEMA-*g*-PAA with a 40% grafting ratio of PAA, shows a more flexible structure. When using MB-40 and POSS-NH_2 to generate MBSs at the interface, it is found that, at different pH values, the measured interfacial tensions are almost the same as the data shown in Figure 2 (Figure S10-S11, the degree of polymerization (DP) of the backbone and, therefore, length of MB-40 and MB-90 are equal). However, due to the significant reduction in the number of PAA side chains in MB-40, the surface coverage has slightly decreased. At a pH of 3.0, nearly full surface coverage (~100%) is reached with the MB-90-based system, while only ~75% surface coverage is obtained with the MB-40-based system (Figure 3a and Video S4). To quantify the mechanical properties of MB-40 and MB-90-based interfacial assemblies, the storage moduli E'(ω) and loss moduli E''(ω) were measured by oscillatory pendant drop tensiometry/rheometry at low concentrations. As shown in Figure 3d-e, for both MB-40 or MB-90-based assemblies, E'(ω) is always higher than E''(ω) in the frequency range from 0.01 to1 Hz, indicating the elastic nature of interfacial assemblies. Moreover, the E'(ω) of the MB-90-based assemblies is significantly higher than that of the MB-40-based assemblies, indicating the more solid-like nature of MB-90-based assemblies.

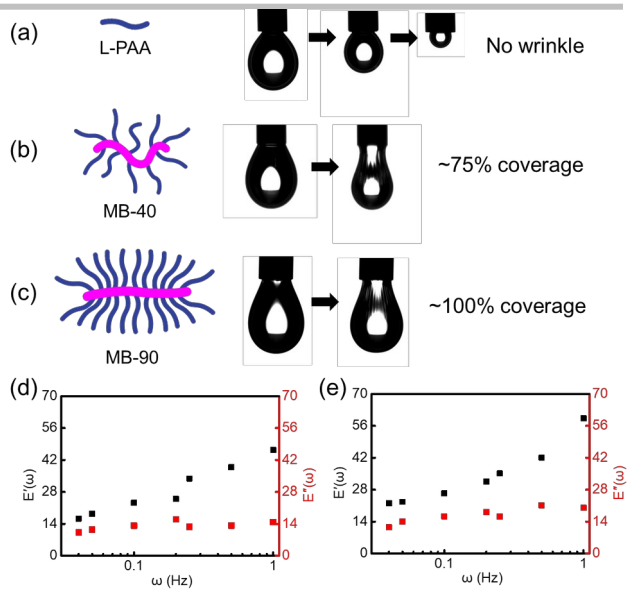

Figure 3. The snapshots of droplet's morphology evolution in an extraction of different oil-water systems including (a) L-PAA@water/POSS-NH_2@toluene, (b) MB-40@water/POSS-NH_2@toluene, and (c) MB-90@water/POSS-NH_2@toluene, [L-PAA] = 0.1 mg mL^{-1} (0.05 mM), [MB-40] = 0. 06 mg mL^{-1} (6 × 10^{-4} mM), [MB-90] = 0.1 mg mL^{-1} (6 × 10^{-4} mM), [POSS-NH_2] = 0.1 mg mL^{-1}, pH = 3.0. Storage and loss dilatational moduli, E′(ω) and E″(ω), of (d) MB-40/POSS-NH_2 assemblies and (e) MB-90/POSS-NH_2 assemblies, [MB-40] = 0.012 mg mL^{-1} (1.2 × 10^{-4} mM), [MB-90] = 0.02 mg mL^{-1} (1.2 × 10^{-4} mM), [POSS-NH_2] = 0.02 mg mL^{-1}, pH = 3.0.

Emulsions were prepared by vigorous mechanical agitation of the MB-90 solution in water with the POSS-NH_2 solution in toluene. Absent POSS-NH_2, emulsions do not form, since the interfacial activity of MB-90 at the toluene-water interface is weak. With POSS-NH_2 dissolved in the toluene, MBSs form *in-situ* and assemble at the interface, significantly reducing the interfacial energy, facilitating the stabilization of emulsions. Figure 4a-c and Figure S13-S14 show the emulsions produced with varying mass ratio of MB-90 to POSS-NH_2 from 0.1/10 to 10/0.1, at a constant 1/1 volume ratio of water and toluene. An evolution of the emulsion from w/o to oil-in-water-oil (o/w/o), then to o/w is observed, as evidenced by the creaming/sedimentation of the dispersed phase and the fluorescent signals from the dispersed/continuous phases. This demonstrates that the hydrophilic-lipophilic balance of MBS at the interface can be effectively adjusted. To the best of our knowledge, this is the first observation of multiple emulsion formation, using MB as the emulsifier, in a one-step process. By varying the water/toluene volume ratio from 1/8 to 8/1 with a 1 mg mL^{-1} solution of MB-90 in the water phase and a 1 mg mL^{-1} solution of POSS-NH_2 in the toluene phase, w/o and o/w emulsions can also be obtained (Figure 4d-g and Figure S16-S17). It should be noted that at a constant water/toluene volume ratio, the size of emulsion droplets are relatively large, and irregular shapes are observed, indicative of the interfacial jamming of MBSs during droplet coalescence, kinetically trapping these structured emulsions (Figure S17). All the emulsions studied show excellent stability

with no obvious morphology change after one month (Figure S15 and Figure S18).

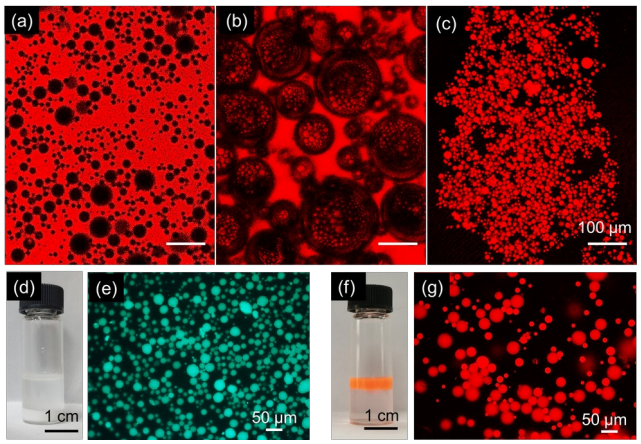

Figure 4. Laser confocal microscope images showing different types of emulsions including (a) w/o, (b) o/w/o, and (c) o/w with different mass ratio of MB-90 to POSS-NH_2 from 10/5 to 10/3, then to 10/0.1 at a constant 1/1 volume ratio of water and toluene. Nile red is loaded in toluene. (d-e) Optical and fluorescent microscope images showing the w/o emulsions at 1/6 volume ratio of water and toluene, with fluorescein isothiocyanate-conjugated dextran (FITC-dextran) loaded in water. (f-g) Optical and Laser confocal microscope images showing the o/w emulsions at 6/1 volume ratio of water and toluene, with Nile red loaded in toluene. From (d) to (g), [MB-90] = 1 mg mL^{-1}, [POSS-NH_2] = 1 mg mL^{-1}, pH = 3.0.

Due to the high interfacial activity and rigid nature of MBSs, the construction of all liquid device with complex shapes was investigated. As shown in Figure S19, by jetting an aqueous MB-90 solution into silicone oil with dissolved POSS-NH_2, Plateau−Rayleigh (PR) instabilities of the aqueous phase are completely suppressed, forming tubular liquids encapsulated with jammed MBSs. Using a 3D printer to control the spatial arrangement of the liquids, spiral tubules of water are produced, which can be used to transport small molecules (e.g., Nile blue) and polymers (e.g., dextran) (Figure 5a-c, Figure S20 and Video S5-S6). Also, by using all-liquid molding, liquid letters spelling “BRUSH” are shown that have exceptional structural stability, and can be reconfigured by external environmental stimuli, e.g., pH (Figure S21 and Video S6). Considering the high structural diversity of MB, tremendous potential applications such as biphasic reactors and chemical separation can be imagined by introducing functional groups into the side-chain or the backbone of MB, which is hard to achieve by using traditional nanoparticle surfactants.

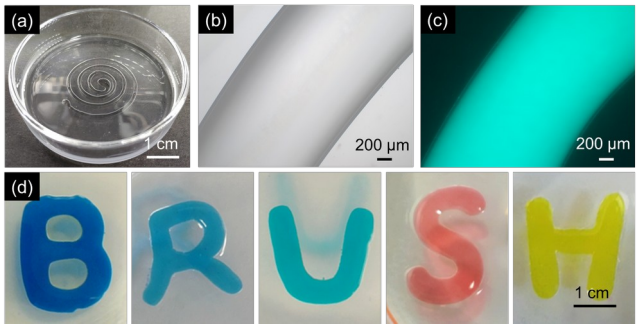

Figure 5. (a-b) Optical microscopy image showing the aqueous spiral produced by all-liquid 3D printing. (c) Fluorescence microscopy image showing the transmission of FITC-dextran in the aqueous spiral. (d) Dyed liquid letters “BRUSH” fabricated by all-liquid molding. [MB-90] = 10 mg mL^{-1}, [POSS-NH_2] = 30 mg mL^{-1}, pH = 3.0.

In summary, we have described a facile approach to stabilize biphasic systems by using MBS, which is formed by the electrostatic interactions between PHEMA-*g*-PAA and POSS-NH_2 at the oil-water interface. The interfacial activity of MBSs can be effectively adjusted by varying the pH or concentration of PHEMA-*g*-PAA/POSS-NH_2 solutions. Using MBSs as emulsifiers, different emulsion types, included o/w, w/o and o/w/o can be easily obtained by varying the molar ratios of PHEMA-*g*-PAA to POSS-NH_2. By taking advantage of the rigid nature and interfacial jamming of MBSs, interfacial assemblies with excellent mechanical properties can be generated, and liquids can be structured to desired shapes using either 3D printing or molding strategy. More importantly, the inherent structural diversity of MBSs opens a new pathway for generating multifunctional all-liquid objects, such as polymersomes and nanoreactors.

Acknowledgements

This work was supported by the National Natural Science Foundation of China (51903011). T.P.R. was supported by the U.S. Department of Energy, Office of Science, Office of Basic Energy Sciences, Materials Sciences and Engineering Division under Contract No. DE-AC02-05-CH11231 within the Adaptive Interfacial Assemblies Towards Structuring Liquids program (KCTR16) and the Army Research Office under contract W911NF-17-1-0003.

Keywords: Liquid-liquid interfaces • molecular brush • jamming • surfactants • structured liquids

[1] H. Chen, W. Li, Y. Lin, L. Wang, X. Liu, X. Huang, *Angew. Chem. Int. Ed.* **2020**, *139*, 17101-17108.
[2] D. Ishikawa, Y. Suzuki, C. Kurokawa, M. Ohara, M. Tsuchiya, M. Morita, M. Yanagisawa, M. Endo, R. Kawano, M. Takinoue, *Angew. Chem. Int. Ed.* **2019**, *58*, 15299-15303.
[3] M. Pera-Titus, L. Leclercq, J.-M. Clacens, F. De Campo, V. Nardello-Rataj, *Angew. Chem. Int. Ed.* **2015**, *54*, 2006-2021.
[4] S.-H. Hu, B.-J. Liao, C.-S. Chiang, P.-J. Chen, I.-W. Chen, S.-Y. Chen, *Adv. Mater.* **2012**, *24*, 3627-3632.
[5] J. E. Norton, I. T. Norton, *Soft Matter* **2010**, *6*, 3735-3742.
[6] J. Wu, G.-H. Ma, *Small* **2016**, *12*, 4633-4648.
[7] B. P. Binks, *Curr. Opin. Colloid Interface Sci.* **2002**, *7*, 21-41.
[8] R. Aveyard, B. P. Binks, J. H. Clint, *Adv. Colloid Interface Sci.* **2003**, *100-102*, 503-546.
[9] H. T. Davis, *Colloids Surf. A Physicochem. Eng. Asp.* **1994**, *91*, 9-24.
[10] M. Cui, T. Emrick, T. P. Russell, *Science* **2013**, *342*, 460-463.
[11] S. Shi, T. P. Russell, *Adv. Mater.* **2018**, *30*, e1800714.
[12] J. Forth, P. Y. Kim, G. Xie, X. Liu, B. A. Helms, T. P. Russell, *Adv. Mater.* **2019**, e1806370.

[13] S. Sun, T. Liu, S. Shi, T. P. Russell, *Colloid. Polym. Sci.* **2021**, *299*, 523-536.
[14] X. Liu, S. Shi, Y. Li, J. Forth, D. Wang, T. P. Russell, *Angew. Chem. Int. Ed.* **2017**, *56*, 12594-12598.
[15] J. Forth, X. Liu, J. Hasnain, A. Toor, K. Miszta, S. Shi, P. L. Geissler, T. Emrick, B. A. Helms, T. P. Russell, *Adv. Mater.* **2018**, *30*, e1707603.
[16] W. Feng, Y. Chai, J. Forth, P. D. Ashby, T. P. Russell, B. A. Helms, *Nat. Commun.* **2019**, *10*, 1095.
[17] C. Huang, J. Forth, W. Wang, K. Hong, G. S. Smith, B. A. Helms, T. P. Russell, *Nat. Nanotechnol.* **2017**, *12*, 1060-1063.
[18] X. Liu, N. Kent, A. Ceballos, R. Streubel, Y. Jiang, Y. Chai, P. Y. Kim, J. Forth, F. Hellman, S. Shi, D. Wang, B. A. Helms, P. D. Ashby, P. Fischer, T. P. Russell, *Science* **2019**, *365*, 264-267.
[19] Y. Chai, A. Lukito, Y. Jiang, P. D. Ashby, T. P. Russell, *Nano Lett.* **2017**, *17*, 6453-6457.
[20] A. Toor, B. A. Helms, T. P. Russell, *Nano Lett.* **2017**, *17*, 3119-3125.
[21] Y. Li, X. Liu, Z. Zhang, S. Zhao, G. Tian, J. Zheng, D. Wang, S. Shi, T. P. Russell, *Angew. Chem. Int. Ed.* **2018**, *57*, 13560-13564.
[22] S. Shi, X. Liu, Y. Li, X. Wu, D. Wang, J. Forth, T. P. Russell, *Adv. Mater.* **2018**, *30*, 1705800.
[23] D. Chen, Z. Sun, T. P. Russell, L. Jin, *Langmuir* **2017**, *33*, 8961-8969.
[24] J. D. Cain, A. Azizi, K. Maleski, B. Anasori, E. C. Glazer, P. Y. Kim, Y. Gogotsi, B. A. Helms, T. P. Russell, A. Zettl, *ACS Nano* **2019**, *13*, 12385-12392.
[25] S. Shi, B. Qian, X. Wu, H. Sun, H. Wang, H. B. Zhang, Z. Z. Yu, T. P. Russell, *Angew. Chem. Int. Ed.* **2019**, *58*, 18171-18176.
[26] J. C. Foster, S. Varlas, B. Couturaud, Z. Coe, R. K. O'Reilly, *J. Am. Chem. Soc.* **2019**, *141*, 2742-2753.
[27] W. F. M. Daniel, J. Burdyńska, M. Vatankhah-Varnoosfaderani, K. Matyjaszewski, J. Paturej, M. Rubinstein, A. V. Dobrynin, S. S. Sheiko, *Nat. Mater.* **2015**, *15*, 183-189.
[28] G. M. Miyake, V. A. Piunova, R. A. Weitekamp, R. H. Grubbs, *Angew. Chem. Int. Ed.* **2012**, *51*, 11246-11248.
[29] M. Abbasi, L. Faust, M. Wilhelm, *Adv. Mater.* **2019**, *31*, e1806484.
[30] R. Verduzco, X. Li, S. L. Pesek, G. E. Stein, *Chem. Soc. Rev.* **2015**, *44*, 2405-2420.
[31] T. L. Hsieh, M. R. Martinez, S. Garoff, K. Matyjaszewski, R. D. Tilton, *J. Colloid Interface Sci.* **2021**, *581*, 135-147.
[32] M. Hu, T. P. Russell, *Mater. Chem. Front.* **2021**, *5*, 1205-1220.
[33] Y. Gao, X. Wu, Z. Xiang, C. Qi, *Langmuir* **2021**, *37*, 2376-2385.
[34] Y. Li, J. Zou, B. P. Das, M. Tsianou, C. Cheng, *Macromolecules* **2012**, *45*, 4623-4629.
[35] G. Xie, P. Krys, R. D. Tilton, K. Matyjaszewski, *Macromolecules* **2017**, *50*, 2942-2950.

Entry for the Table of Contents

Insert graphic for Table of Contents here.

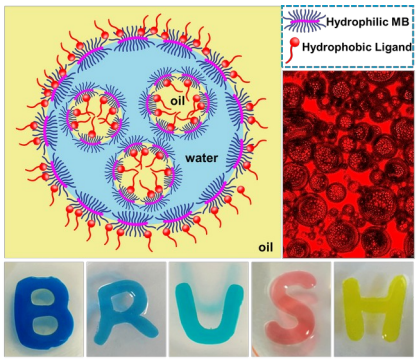

By taking advantage of the cooperative assembly between hydrophilic molecular brushes and hydrophobic oligomeric ligands, the formation, assembly and jamming of a new type emulsifier, termed molecular brush surfactant (MBS), is present. With MBSs at the oil-water interface, stable emulsions including o/w, w/o and o/w/o can be easily prepared in a one-step process. Moreover, when jammed, the binding energy of MBSs at the interface is sufficiently strong to allow the stabilization of liquids in highly nonequilibrium shapes, e.g., liquid letters, producing an elastic film at the interface with exceptional mechanical properties.